Published in final edited form as:
Neuroimage. 2014 November 15; 102(0 2): 646–656. doi:10.1016/j.neuroimage.2014.08.028.

Domain-General and Domain-Specific Functional Networks in Working Memory

Dawei Li[1], **Shawn E. Christ**[2], and **Nelson Cowan**[2]

[1]Center for Cognitive Neuroscience, Duke University

[2]Department of Psychological Sciences, University of Missouri

Abstract

Working memory (WM) is a latent cognitive structure that serves to store and manipulate a limited amount of information over a short time period. How information is maintained in WM remains a debated issue: it is unclear whether stimuli from different sensory domains are maintained under distinct mechanisms or maintained under the same mechanism. Previous neuroimaging research on this issue to date has focused on individual brain regions and has not provided a comprehensive view of the functional networks underlying multi-domain WM. To study the functional networks involved in visual and auditory WM, we applied constrained principal component analysis (CPCA) to a functional magnetic resonance imaging (fMRI) dataset acquired when participants performed a change-detection task requiring them to remember only visual, only auditory, or both visual and auditory stimuli. Analysis revealed evidence of both [1] domain-specific networks responsive to either visual or auditory WM (but not both), and [2] domain-general networks responsive to both visual and auditory WM. The domain-specific networks showed load-dependent activations during only encoding, whereas a domain-general network was sensitive to WM load across encoding, maintenance, and retrieval. The latter domain-general network likely reflected attentional processes involved in WM encoding, retrieval, and possibly maintenance as well. These results do not support the domain-specific account of WM maintenance but instead favor the domain-general theory that items from different sensory domains are maintained under the same mechanism.

Keywords

working memory; fMRI; functional network; constrained principal component analysis; domain-general; domain-specific

Working memory (WM) is a latent cognitive structure that serves to store and manipulate a limited amount of information over a short time period (Baddeley & Hitch, 1974; Cowan,

Address correspondence to: Nelson Cowan Department of Psychological Sciences University of Missouri 210 McAlester Hall Columbia, MO 65211 Tel. 573-882-4232 CowanN@missouri.edu.

1995). WM is crucial for a number of advanced cognitive processes, such as language, reasoning, and decision making. How items are maintained in WM, however, remains a debated issue. Some researchers hold that items from different sensory domains, such as vision and audition, are stored in relatively separate WM stores and maintained under distinct mechanisms (Baddeley & Hitch, 1974; Cocchini et al., 2002). This account is referred to as a domain-specific view of WM storage. In contrast, although acknowledging the existence of domain-specific stores in WM, others (e.g. Cowan, 1995; Kane et al., 2004; Saults & Cowan, 2007) argue for the existence of a unitary WM maintenance system that retains stimuli from different sensory domains. This account is referred to as a domain-general view of WM storage.

The domain-specific and domain-general theories give rise to distinct predictions of the patterns of brain activity associated with WM maintenance. For example, the domain-specific view predicts that different brain regions are involved in WM maintenance of stimuli from different domains. Consistent with this view, Smith and Jonides (1997) found lateralized activation of the left and right prefrontal cortex during maintenance of verbal versus spatial information, respectively. Additional support comes from studies suggesting that the dorsolateral prefrontal cortex is involved in spatial WM maintenance whereas the ventrolateral prefrontal cortex is involved in nonspatial object WM maintenance (Courtney et al., 1996; Haxby et al., 1994; Ungerleider et al., 1998).

In contrast to the domain-specific view, the domain-general view predicts that in addition to brain regions specific for individual domains, a common brain region (or regions) is consistently involved in WM maintenance regardless of stimulus domain. This region (or regions) may serve as either a storage system for domain-general information or an attention system that directs attention to item-specific information during WM maintenance. Evidence consistent with this view comes from our recent study (Cowan et al., 2011), which found that a region in the intraparietal sulcus (IPS) was consistently activated during the maintenance of stimuli in WM regardless of whether it was visual or auditory in nature. Overlapping brain regions have also been found to activate for verbal and spatial WM (Chein et al., 2011), visual and verbal WM (Majerus et al, 2010), as well as verbal and tonal WM (Koelsch et al., 2009).

As detailed above, previous neuroimaging studies have failed to resolve the domain-specific versus domain-general debate regarding the nature of WM storage. Of note, the majority of these studies have relied on univariate statistical approaches. Univariate approaches, such as the general linear model, are focused on the time series of each voxel independently and disregard the correlation between voxels. It can be argued, however, that the correlation between spatially distant brain voxels is a critical feature of fMRI datasets and reflects important information about the functional networks underlying cognitive tasks, which would not otherwise be evident using a univariate approach alone. Multivariate approaches take into account such inter-voxel correlations and thus may provide a more comprehensive view of the functional networks underlying WM.

An exploratory multivariate approach, constrained principal component analysis (CPCA), is used in this study to investigate the domain-general and domain-specific functional networks

in WM. CPCA combines principal component analysis (PCA) with multivariate multiple regression and has been used in neuroimaging studies on WM (Metzak et al., 2011, 2012; Woodward et al., 2006, 2013; for a complete introduction of the theory and applications of CPCA, see Hunter & Takane, 2002; Takane & Hunter, 2001). CPCA has several advantages over the other multivariate approaches. First, it is an exploratory whole-brain analysis approach and unlike other approaches such as dynamic causal modeling and structural equation modeling, does not require a priori extraction of a specified group of regions of interest. Second, unlike some other exploratory approaches such as PCA and independent component analysis, CPCA excludes the task-irrelevant variance and operates on the task-related variance in a data set. Finally, a finite impulse response (FIR)-based CPCA (Metzak et al., 2012), which is used in this analysis, is capable of tracking the dynamics of functional network over the entire trial. This is especially important in WM studies, in which the successive encoding and maintenance periods appear to recruit distinct functional networks (Woodward et al., 2006).

Application of multivariate techniques such as CPCA to fMRI data has already yielded valuable insights into other WM-related questions. For example, Woodward and colleagues (2006) identified separate load-dependent functional networks for WM encoding and maintenance and found strong negative correlation between the encoding and maintenance networks, which indicates complementary processes underlying WM encoding and maintenance. Importantly, past multivariate fMRI studies of WM (e.g., Abe et al., 2007; Chang et al., 2007; Cohen et al., 2012; Edin et al., 2007; Edin & Klingberg, 2009; Fiebach, Rissman, & D'Esposito, 2006; Gazzaley et al., 2004, 2007; Habeck et al., 2012; Hampson et al., 2006, 2010; Honey et al., 2002; Kim et al., 2012; Kondo et al., 2004a, 2004b; Kuo et al., 2011; Lenartowicz & McIntosh, 2005; Ma et al., 2012; Mayer et al., 2009; Palva et al., 2010; Payne & Kounios, 2009; Rissman et al., 2008; Schlösser et al., 2006; Sundermann & Pfleiderer, 2012) have used stimuli from only one sensory domain. Consequently, their potential value for answering the question of a domain-general versus domain-specific WM storage system is extremely limited.

In the present study, we bring multivariate techniques to bear on the question of whether the WM storage system is better conceptualized as a domain-specific or domain-general mechanism. Specifically, we applied CPCA to an existing fMRI dataset (Experiment 2 in Cowan et al., 2011) in which participants performed a task requiring them to remember stimuli from a single domain (i.e., only visual or only auditory) or multiple domains (both visual and auditory). The domain-specific theory would predict that, when both visual and auditory stimuli are used in the task, the WM storage system would recruit multiple functional networks, each of which includes specific brain areas for visual or auditory processing and shows distinct activity patterns for visual and auditory WM. In contrast, the domain-general theory would predict that in addition to domain-specific functional networks for visual or auditory process, a single functional network would be recruited for both visual and auditory WM.

Method

For this study, we re-analyzed the data from Experiment 2 of Cowan et al. (2011), and a detailed description of the experiment can be found in that article. A brief summary of the experimental tasks is presented below.

Participants

Sixteen participants (7 male), ranging from 18 to 20 years old, were included in the analysis. All participants were college students at the University of Missouri. Another participant was not included in the analysis because of excessive head motion.

Behavioral Procedure

Figure 1 shows the procedure of the experiment. The participants performed a change-detection task, in which they remembered a few visual and/or auditory items for several seconds. Each trial started with a 1000 ms fixation, after which the participants were presented two auditory letters (2A), two visual colored squares (2V), two visual colored squares plus two auditory letters (2V2A), or four visual colored squares (4V), for 1500 ms. For conditions including auditory letters, the letters were presented sequentially, with each letter lasting approximately 500 ms with a 250 ms inter-stimulus interval. For conditions including colored squares, the colored squares were presented simultaneously on the screen for 1500 ms. Presentation of the to-be-remembered stimuli was following by a 1000 ms blank display and a 500 ms visual and acoustic mask in order to eliminate traces of sensory memory.

The sensory mask was followed by an 8000 ms retention interval, which consisted of a blank display. Next, a single test item was presented, and the participants were instructed to press a button to indicate whether this test item was the same as the remembered item at the same spatial location or verbal serial position as the test item, or was different from any item that they remembered. The test stimulus was presented for 1000 ms, after which a “?” appeared on the screen. The participants had 3000 ms to respond to the test, after which feedback was provided. Additionally, to discourage verbal rehearsal, the participants were required to continuously whisper the word “the” at a rate of twice per second from the trial onset until the test stimulus appeared. Each trial lasted 18 s. Each participant performed 10 fMRI runs, and each run included 16 trials (4 trials for each condition).

Neuroimaging Data Acquisition

The neuroimaging data was acquired with a 3T Siemens Trio scanner at the Brain Imaging Center in Department of Psychological Sciences at the University of Missouri. High-resolution T1- and T2-weighted structural images were collected for use in later volume registration. Ten functional runs, each lasting 195 TRs, were then collected with a T2*-weighted echo planar pulse sequence (TR = 2000 ms, TE = 30 ms, resolution = 4 mm3, 32 axial slices).

Neuroimaging Data Preprocessing

The fMRI data were preprocessed using SPM8 (http://www.fil.ion.ucl.ac.uk/spm/software/spm8/). The preprocessing included slice-timing correction, head motion correction, co-registration of functional and anatomical images, spatial normalization into the Montreal Neurological Institute (MNI) space, resampling to isotropic 2-mm voxels, and spatial smoothing using a 6 mm FWHM Gaussian filter.

Functional Network Analysis

The univariate analysis method and results have been reported in Cowan et al. (2011). Below we describe the functional network analysis method.

The preprocessed data were analyzed using CPCA implemented in the fMRI-CPCA toolbox (version 1.1.0.06, http://www.nitrc.org/projects/fmricpca), which combines principal component analysis (PCA) with multivariate multiple regression analysis. As a first (and critical) step, CPCA performs a multivariate multiple regression on the entire fMRI dataset in order to extract a relatively pure estimate of task-related variance. The goal of this process is to remove nuisance variance related to all task-irrelevant factors such as head movement, MR signal drift over time, and any cognitive process unrelated to timings of the task. In the multivariate multiple regression, two matrices are generated: a data matrix *Z* and a design matrix *G*. The data matrix *Z* contains the standardized BOLD signal, with each row representing one participant-specific volume and each column representing a voxel. The design matrix *G* contains timing of the experimental task conditions, with each row representing one participant-specific volume and each column representing one participant- and condition- and time-point-specific predictor. With respect to the current analysis, the resulting matrix *Z* had 30,880 rows and 189,368 columns, and the matrix *G* had 30,880 rows and 1024 columns. A finite impulse response (FIR) model was used to estimate the BOLD signal change over post-stimulus time. BOLD response for each condition and each participant was modeled by 16 predictors that cover a time duration of 32 seconds, with the first predictor corresponding to the trial onset corresponding to the 1000 ms fixation. For each column of the *G* matrix, a value of 1 was assigned to the rows that are to be estimated by this predictor, and a value of 0 was assigned to the remaining rows.

Multivariate least-square linear multiple regression is performed in which the data matrix Z is regressed on the design matrix *G*:

$$Z=GC+E,$$

in which *C* contains each voxel's beta weights for each experimental task condition in each participant, and *E* is the error matrix. The product of *GC* reflects the variance relevant to the experimental design.

The second step of CPCA is to perform PCA on the *GC* matrix. This procedure identifies a set of orthogonal variables called principal components that explain a relatively large amount of variance in the data set. The number of selected principal components is usually

less than the number of the original variables, and thus the dimensionality of the data set is reduced. The procedure involves generalized singular value decomposition of *GC*:

$$UDV' = GC,$$

in which *D* is a diagonal matrix with nonnegative real numbers, known as singular values, on the diagonal, *U* is a matrix containing the left-singular vectors, and *V* is a matrix containing the right-singular vectors. Each column of the *V* matrix represents a functional network and could be rescaled using the singular values in *D (VD)* and be mapped on a brain template to show the involved brain regions. Given that the original components represented by the matrix *VD* showed reasonable spatial patterns, the matrix *VD* was not rotated in this study.

Condition-specific predictor weights are calculated in matrix *P* (*U* = *GP*). The predictor weights in the matrix *P* represent the contribution of each predictor to each principal components for each participant, and thus allow for statistical tests of the effects of WM load condition and time points on the functional networks represented by the principal components.

Results

Four primary principal components were selected based on visual examination of the scree plot. The four components each accounted for 41.69%, 11.17%, 4.90%, and 4.19%, respectively, of the task-related variance. We believe that these components reflect, respectively, (1) domain-general encoding; (2) articulatory suppression, which was used in all conditions; (3) domain-general attention involved in WM encoding, maintenance, and retrieval; and (4) domain-specific visual encoding. Another important component, reflecting domain-specific auditory encoding, showed up sixth in the analysis and will also be described.

The functional networks represented by the two domain-general components, Components 1 and 3, are shown in Figure 2A and C, respectively. The predictor weights of Components 1 and 3, which depict the contribution of each component to the task conditions over time, are plotted in Figure 2B and D, respectively. The functional network represented by Component 2 is shown in Figure 3A, and its predictor weights are plotted in Figure 3B. The functional networks represented by the two domain-specific components, Components 4 and 6, are shown in Figure 4A and C, respectively. The predictor weights of Components 4 and 6 are plotted in Figure 4B and D, respectively. Figure 5C1, C3, C4, and C6 shows results of the post hoc Newman-Keuls tests comparing the predictor weights of each two memory conditions at each time point for Components 1, 3, 4, and 6, respectively.

In all figures of time courses of predictor weights, the WM encoding, late maintenance, and response periods were marked with yellow, red, and blue rectangles, respectively, after correcting for 6s delay of the hemodynamic response function. The early maintenance period was influenced by carryover signal from the encoding period and was thus not marked in the figures and was not considered in interpretation of results.

Supplemental tables 1, 2, 3, and 4 contain the coordinates, Brodmann area, and size (mm^3) of each brain region for Components 1, 3, 4, and 6, respectively. (As detailed below, Component 2 appears to have limited theoretical significance and therefore was excluded from the aforementioned tables.)

Component 1: Domain-General Encoding

The Figure 2A shows the functional network represented by Component 1. The functional network associated with component 1 consisted of several brain regions including bilateral lateral occipital cortex, left lingual gyrus, bilateral superior IPS, bilateral precuneus, bilateral superior temporal gyrus, right fusiform gyrus, left precentral gyrus, right premotor cortex, left dorsolateral prefrontal cortex, bilateral inferior frontal gyrus, bilateral medial frontal gyrus, bilateral anterior cingulate cortex, bilateral insula cortex, bilateral thalamus, and bilateral dorsal striatum. All brain regions showed positive loading values.

Figure 2B shows the predictor weights for each WM load condition. Visual inspection of the plots showed that this network had the highest predictor weights during WM encoding, which seem to depend on the number of items to be encoded into WM regardless of sensory domain. A two-way repeated measure ANOVA with WM load conditions (2A, 2V, 2V2A, and 4V) and time points (1 to 16) as within-subject factors showed a significant main effect of time points, $F(15, 225) = 5.77$, $p < .001$, $\eta_p = .28$, as well as a significant interaction of WM load condition by time points, $F(45, 675) = 1.87$, $p < .001$, $\eta_p = .11$. The main effect of time points was mainly due to the increased predictor weights during encoding compared with those during maintenance and probe (Figure 2B).

Post hoc Newman-Keuls test of the interaction effect revealed that the 2A and the 2V conditions showed almost identical predictor weights across the trial, and that the 2V2A and the 4V conditions also showed almost identical predictor weights across the trial (Figure 5C1). Importantly, the interaction was caused by higher predictor weights for the 2V2A condition versus the 2V and the 2A conditions, as well as higher predictor weights for the 4V condition versus the 2V condition during the encoding phase. Thus, Component 1 showed such a pattern that conditions with four items had higher predictor weights than conditions with two items, regardless of sensory domains, during WM encoding. This pattern suggests that this brain network is sensitive to domain-general WM load during encoding. The 4V versus 2A contrast during encoding was not significant, though the means were in the anticipated order.

Component 2: Articulatory Suppression

Figure 3A shows the functional network represented by Component 2. Both positive and negative brain regions were included in this network. The positive brain regions included bilateral inferior frontal gyrus, bilateral middle frontal gyrus, right superior and middle temporal gyrus, bilateral caudate nucleus, and right inferior temporal gyrus. The negative brain regions included left postcentral gyrus, as well as areas around the brain and near the medial line. Importantly, there were no differences between conditions in this component (Figure 3B). This limits its theoretical significance; it is presented here only because it accounts for the second-highest amount of variance overall. It is likely to represent the brain

activity related to articulatory suppression (whispering “the” repeatedly), which was carried out from the beginning of each trial through the manual response to prevent covert verbal rehearsal, but was not carried out between trials. There also were some indications of movement artifact from this suppression task (Birn et al., 2005; Yetkin et al., 1996) that had been subtracted out for univariate analyses reported by Cowan et al. (2011).

Component 3: Domain-General Attention

Figure 2C shows the functional network represented by Component 3. Both positive and negative brain regions were included in this network. The positive brain regions included left IPS and bilateral precentral gyrus. The negative brain regions included bilateral posterior cingulate cortex, left inferior parietal lobule, bilateral occipital cortex, bilateral postcentral gyrus, bilateral superior frontal gyrus, bilateral ventral cingulate cortex, and bilateral ventral medial prefrontal cortex.

Visual inspection of the predictor weight plots in Figure 2D suggests that this network is sensitive to multimodal WM load during encoding, maintenance, and retrieval periods. A twoway repeated measure ANOVA with WM load conditions (2A, 2V, 2V2A, and 4V) and time points (1 to 16) as within-participant factors showed a significant main effects of WM load conditions, $F(3, 45) = 10.03$, $p < .001$, $\eta_p = .40$, and time points, $F(15, 225) = 16.91$, $p < .001$, $\eta_p = .53$. As illustrated in Figure 5C3, the main effect of WM load conditions was due to higher overall predictor weights for the 2V2A and the 4V conditions compared with those for the 2A and the 2V conditions, as well as higher overall predictor weights for the 4V condition compared with those for the 2V2A condition. The main effect of time points was due to an “M”-shaped time course in which the predictor weights were higher during encoding and probe and lower during maintenance (Figure 2D).

The interaction between WM load conditions and time points was also significant, $F(45, 675) = 5.79$, $p < .001$, $\eta_p = .28$. This interaction reflected changes of WM load effect across different periods of WM, and it is mostly driven by a large domain-general load effect during encoding that persisted during maintenance, and a much smaller load effect during retrieval. Importantly, both the 2V2A and the 4V conditions showed significantly higher predictor weights than the 2A and the 2V conditions at most time points representing WM encoding, maintenance, and retrieval (Figure 5C3). This fact suggests that Component 3 was involved in domain-general processes in all periods of WM. Adding the fact that most brain regions showing negative loading values in Component 3 are part of the default mode network which typically shows negative activation during attention-demanding tasks compared with baseline (Buckner et al., 2008), Component 3 was likely to be involved in domain-general attentional processes in WM. These attentional processes appear to be manifested as transient peaks of activations during encoding and retrieval, as well as sustained activation during maintenance. We argue that this component was likely recruited in different types of attention-demanding tasks in different periods of WM such as: feature integration, object binding, memory consolidation during encoding, direction of attention to domain-specific stores during maintenance, and retrieval of information just prior to response.

Component 4: Domain-Specific Visual Encoding

Figure 4A illustrates the functional network represented by Component 4. Both positive and negative brain regions were included in this network. The positive brain regions included bilateral posterior IPS, bilateral precuneus, left occipital cortex, left precentral gyrus, left dorsolateral prefrontal cortex, bilateral medial frontal gyrus, and bilateral cerebellum. The negative brain regions included bilateral supramarginal gyrus, right inferior frontal gyrus, bilateral ventral anterior cingulate cortex, bilateral insula, and left parahippocampal gyrus.

Visual inspection of the predictor weights plots showed that this brain network is sensitive to visual load during WM encoding but not maintenance and retrieval (Figure 5C3). A two-way repeated measure ANOVA with WM load conditions (2A, 2V, 2V2A, and 4V) and time points (1 to 16) as within-participant factors showed a significant main effects of WM load conditions, $F(3, 45) = 8.07$, $p < .001$, $\eta_p = .35$, and time points, $F(15, 225) = 9.63$, $p < .001$, $\eta_p = .39$. The main effect of WM load conditions was primarily due to higher overall predictor weight for the 4V condition compared with those for the other three conditions (Figure 5C3). The main effect of time points appears to be due to elevated predictor weights during WM encoding and maintenance, but not during retrieval (Figure 5C3).

The interaction between WM load conditions and time points was also significant, $F(45, 675) = 14.73$, $p < .001$, $\eta_p = .50$. Post hoc Newman-Keuls test showed that the interaction was mainly due to differences of predictor weights caused by visual load during the encoding period. During the encoding period represented by approximately time points 4 and 5, the predictor weights for the 4V condition were higher than those for the 2V2A and the 2V condition, which in turn were higher than those for the 2A condition (Figure 5C4). After encoding, the predictor weights for different WM load conditions converged and showed smaller differences. Although the 4V condition continued to show higher predictor weights than the 2V condition throughout the maintenance window, this load effect did not generalize to the other contrasts, such as [4V – 2V2A], [2V2A – 2A], and [2V – 2A], during the maintenance period. It thus seems likely that this neural network is responsible for processing visual information during WM encoding.

Component 6: An Additional Component-of-Interest: Domain-Specific Auditory Encoding

In order to identify additional components that may have shown insightful patterns but did not explain a relatively large amount of variance, we extracted ten components in a separate analysis. Besides Components 1 to 4, only Component 6 showed WM load-dependent predictor weights. Therefore, another analysis was conducted in which six components were extracted. Components 1 to 4 revealed by this analysis were identical to Components1 to 4 described in the previous sections. Component 6 in this analysis accounted for 2.3% of the task-related variance. Figure 4C shows the functional network represented by Component 6. This functional network included both positive and negative brain regions. The positive brain regions included bilateral superior temporal gyrus and bilateral inferior frontal gyrus. The negative brain regions included bilateral precentral and postcentral gyrus, left fusiform gyrus, left thalamus, and left parahippocampal gyrus.

Figure 4D shows the predictor weights for each WM load condition in Component 6. Visual inspection of the plots shows that this network was sensitive to auditory load during only the encoding period. A two-way repeated measure ANOVA with WM load conditions (2A, 2V, 2V2A, and 4V) and time points (1 to 16) as within-participant factors showed a significant main effects of WM load conditions, $F(3, 45) = 17.91$, $p < .001$, $\eta_p = .54$, and time points, $F(15, 225) = 7.66$, $p < .001$, $\eta_p = .34$. The main effect of WM load conditions was due to higher overall predictor weights for the 2A and the 2V2A conditions compared with those for the 2V and the 4V conditions (Figure 5C6). The main effect of time points was due to elevated average predictor weights during the encoding period (Figure 4D).

The interaction between WM load conditions and time points was also significant, $F(45, 675) = 21.08$, $p < .001$, $\eta_p = .58$. Post hoc Newman-Keuls test showed that the interaction was primarily due to higher predictor weights for the 2A and the 2V2A conditions than those for the 2V and the 4V conditions during only the encoding period (Figure 5C6). This functional network is therefore likely to be responsible for processing auditory information during WM encoding.

Discussion

In this study we investigated functional networks underlying a multimodal change-detection experiment. An exploratory multivariate data analysis method, CPCA, was used to extract functional networks underlying the WM task.

CPCA revealed distinct brain networks sensitive to domain-general versus domain-specific processes. On one hand, two components demonstrated characteristics consistent with domain-general load dependency: Component 1 was sensitive to both visual and auditory loads during only the encoding period, and Component 3 was sensitive to both visual and auditory loads throughout the trial. On the other hand, the results for two other components were consistent with domain-specific load dependency: Component 4 was sensitive to visual load (but not auditory load) during the encoding period, and Component 6 showed dependency on auditory load (but not visual load) during the encoding period. These findings are consistent with the assertion that different functional networks are involved in domain-general and domain-specific processes in the WM task.

The two domain-general components, Components 1 and 3, showed different patterns of predictor weights and consisted of different brain regions. Component 1 was sensitive to visual and auditory load during only the encoding period and included primary sensory regions as well as several association areas including the IPS, the precuneus, the dorsolateral prefrontal cortex, the anterior insula, the premotor cortex, and the dorsal anterior cingulate cortex. Most of these brain regions, such as the precuneus, the dorsolateral prefrontal cortex, the premotor cortex, and the dorsal anterior cingulate cortex, are frequently found to be active during WM encoding (Cairo et al., 2004; Habeck et al., 2005; Woodward et al., 2006). Moreover, Component 1 showed the largest predictor weights during WM encoding. Therefore, this component seems to represent a functional network for domain-general encoding. Component 1 also showed a small peak of predictor weights during WM retrieval equally for all memory conditions, which might reflect encoding of test stimuli.

In contrast, Component 3 was sensitive to visual and auditory loads throughout the trial. This component was consisted of both negative and positive regions. Most of the negative brain regions overlapped with the default mode network which shows deactivation during attention-demanding tasks compared to rest (Buckner et al., 2008). In Component 3, these default mode brain regions showed more deactivation in 4-item conditions, which were more difficult and likely recruited more attention resource than 2-item conditions (Cowan et al., 2011), regardless of sensory domain. This fact supports the role of Component 3 in domain-general attention processes in WM. Another piece of evidence supporting this role of Component 3 is that during WM maintenance, the 2V2A, 2V, and 2A conditions had similar predictor weights, which were significantly smaller than predictor weights in the 4V condition (Figure 2D, 6B). This pattern is consistent with behavioral results that participants had similar accuracy rates in the 2V2A (0.95±0.04), 2V (0.94±0.06), and 2A (0.95±0.07) conditions, which were lower than that in the 4V condition (0.86±0.08) (Cowan et al., 2011). These results suggest that the 4V condition was the most difficult and attention-demanding, and that the time course of Component 3 during WM maintenance reflected the amount of attention resource involved in the task, which supports the argument that Component 3 reflects domain-general attention processes.

Component 3 also consisted of several brain regions with positive loading values, among which was a subregion within the left anterior IPS (MNI coordinates: −42, −40, 42; see Figure 3C, expanded region). Interestingly, in the univariate analysis of the same data, another subregion in the left anterior IPS was also identified to be sensitive to bimodal memory load during WM maintenance (Talairach coordinates: −27, −46, 31; see Cowan et al., 2011, Figure 3). After MNI-to-Talairach conversion (Lacadie et al., 2008; http://noodle.med.yale.edu/~papad/mni2tal/), the IPS region in this analysis shows center coordinates of (−42 −38 40), which appears to be spatially separate from the IPS region in Cowan et al. (2011) (−27, −46, 31). It should be noted, however, that interpretations of such a comparison require extra caution given the different processing streams and registration algorithms used to derive these brain regions, as well as less-than-ideal conversion algorithms between MNI and Talairach spaces. Therefore, it is unclear whether these two IPS subregions represent the same neural clusters or two different ones. Only a small region within the precentral gyrus was found to be positively connected with the left anterior IPS in this network, although there were several negative brain regions as noted. When we relaxed the criterion to examine the brain regions with top 10% loading values, however, we found that the positive brain regions also included bilateral dorsal anterior cingulate cortex, which has been suggested to be part of the executive control attention network (Posner & Petersen, 1990; Petersen & Posner, 2012) and to modulate activities in the lateral frontal and the parietal regions (Bush et al., 2000). It thus seems that the left anterior IPS, the dorsal anterior cingulate cortex, the precentral gyrus, and regions in the default mode network form a network responsible for domain-general attention processes in WM.

Time course of Component 3 shows that this domain-general attention network exhibited an M shape with two peaks at encoding and retrieval and persisted activity during maintenance. Thus, Component 3 clearly reflected attentional processes in encoding and retrieval, and possibly in maintenance as well. The peaks at encoding and retrieval suggest that these periods might require more attention resources than WM maintenance because they both

consist not only of WM but also of some other processes, such as perception and motor response, respectively. The absence of a peak during maintenance might reflect sustained maintenance activity which typically does not involve a sharp increase of neural activity. Despite the absence of a peak, the role of Component 3 in maintenance could possibly be supported by two points. First, the time course of Component 3 showed a domain-general load effect during maintenance, suggesting its active role in maintenance. Importantly, the load effect during maintenance showed a different pattern (4V > 2V2A = 2V = 2A) from that during encoding (4V = 2V2A > 2V = 2A) (Figure 2D & 5C3), suggesting that the load effect during maintenance was not just carryover signal from encoding but reflected attention processes different from those in encoding. Second, as discussed in the above paragraphs, levels of predictor weights of Component 3 during maintenance (4V > 2V2A = 2V = 2A) were consistent with accuracy rates. This fact indicates that time course of Component 3 during maintenance was not random fluctuation but was indicative of behavioral performance. Thus, although these points cannot be considered as direct evidence, it is possible that Component 3 was involved in domain-general maintenance as well, not just encoding and retrieval. More specifically, during maintenance, this domain-general network might reflect the focus of attention which directs attention to item information held in domain-specific stores (Harrison & Tong, 2009; Ruchkin et al., 2003). In sum, we propose that Component 3 was likely to be involved in various attention-demanding processes in all periods of WM, such as feature integration, object binding, and memory consolidation in encoding, direction of attention to domain-specific stores in maintenance, and retrieval of information in the period just preceding a response. It should be noted, however, that the clearer evidence is necessary to provide more direct support of this network's role in WM maintenance.

Unlike the domain-general components, the two domain-specific components, Components 4 and 6, showed similar patterns of predictor weights: both components were sensitive to domain-specific load during the encoding period. Component 4 was sensitive to visual load during encoding and included the lateral occipital cortex and the posterior IPS. The lateral occipital cortex is widely accepted to be responsible for visual object recognition (Grill-Spector et al., 2001). The posterior IPS is spatially distinct from the anterior IPS discovered in Component 3. The posterior IPS has been reported to be sensitive to visual object complexity (Xu & Chun, 2006), to be dependent on visual load in a perceptual task with no memory requirements (Mitchell & Cusack, 2008), and to be structurally connected to the superior occipital lobe (Uddin et al., 2010). Interestingly, a similar posterior IPS region was previously proposed to be responsible for visual WM maintenance (Todd & Marois, 2004). Combined with our findings, we could suggest that this region carries visual-specific encoding information that under some circumstances can also contribute to visual working memory. An alternative possibility is that different subregions within the posterior IPS, which are indistinguishable with current experimental paradigms and techniques, are involved in WM encoding versus maintenance.

Component 6 was sensitive to auditory load and consisted of bilateral superior temporal gyrus and inferior frontal gyrus. The superior temporal gyrus is responsible for auditory processing (Demonet et al., 1992). The left inferior frontal gyrus is important for verbal comprehension and is frequently reported to be active during verbal WM encoding and

maintenance (Cohen et al., 1997; Nixon et al., 2004). The latter region, however, was not necessarily recruited during verbal WM maintenance in this study, given that Component 6 was not sensitive to auditory load during the maintenance period.

It is thus clear that different functional networks were responsible for domain-general and domain-specific processes in WM. On one hand, the domain-specific networks showed load-dependent patterns during only the encoding period, suggesting their roles in domain-specific encoding. On the other hand, the domain-general network represented by Component 1 showed load-dependent patterns during the encoding period, whereas the domain-general network represented by Component 3 showed load-dependent patterns throughout the entire trial.

WM encoding recruited both domain-specific (Components 4 and 6) and domain-general networks (Component 1). These networks are likely to be involved in both perceptual encoding and WM consolidation. One possibility is that the domain-specific networks are involved in perceptual encoding, and that the domain-general network subsequently consolidates the perceptual representations into WM. This possibility is partly supported by the fact that the onset of the load effect was earlier in the domain-specific networks than in the domain-general networks (Figure 5C1, C4, C6). Another piece of evidence is that Components 4 and 6 include mostly posterior sensory regions, and that Component 1 includes not only sensory but also association regions. None of the above evidence, however, is conclusive enough to exclude the possibility that Components 4 and 6 also reflected memory-related encoding. It is unclear whether these two components will show up in a pure perceptual task without memory requirement. Elucidation of the exact functions of these networks, therefore, requires more investigation.

In contrast to WM encoding, WM maintenance appears to recruit only a domain-general network represented by Component 3. This network showed domain-general load dependency during all periods of WM and likely reflected attention processes involved in WM. During maintenance, this network might direct attention to item information held in domain-specific stores. Although no domain-specific brain network was involved in WM maintenance in this analysis, this does not necessarily imply that WM storage does not recruit any stimulus-specific process. In fact, a few recent studies used multi-voxel pattern analysis to decode the BOLD signal and found that the posterior sensory regions showed stimulus-specific activity patterns during WM maintenance (Harrison & Tong, 2009; Lewis-Peacock & Postle, 2012; Riggall & Postle, 2012). These studies proposed that the posterior sensory regions function in a sub-threshold manner which cannot typically be detected by traditional analysis methods. It is thus possible that the posterior sensory regions receive attentional regulation from the domain-general attention network represented by Component 3. In this way, lower-level stimulus-specific information is well preserved in WM. The notion of using attention as a process to refresh representations, keeping them active in memory, is supported by previous behavioral research (e.g., Camos, Mora, & Oberauer, 2011) and neuroimaging research (e.g., Raye et al., 2007).

Interestingly, several subregions within the IPS were functionally connected to different brain regions and showed different properties in this study (Figure 6). Component 3

included a small region within the left anterior IPS that worked with several frontal regions and showed domain-general WM load dependency during multiple stages in the WM tasks. Component 4 included a region within bilateral posterior IPS that was functional connected to primarily the lateral occipital cortex and was sensitive to only visual load during the encoding periods. Component 1 included a region within bilateral posterior IPS that was functionally connected to both posterior sensory regions and multiple frontal and subcortical regions and was sensitive to domain-general load during only the encoding period. Importantly, these three IPS subregions showed little overlap, consistent with the view that the IPS consists of multiple subregions each with distinct functions (Culham & Kanwisher, 2001; Xu & Chun, 2006). Figure 6 shows these three IPS subregions in the left hemisphere. This finding is also supported by a resting-state and structural connectivity study by Uddin and colleagues (Uddin et al., 2010), which partitioned the IPS into three parts and found that the two anterior parts showed greater resting-state functional connectivity and structural connectivity with prefrontal regions, and that the posterior part showed greater resting-state functional connectivity and structural connectivity with extrastriate visual areas. The exact segregations of the IPS as well as the functions of different segregations, however, still warrant further investigation.

In summary, the present application of CPCA to data from a multi-modal working memory fMRI study revealed multiple functional networks. By using simultaneous visual and auditory stimuli in a single trial, this study allowed for evaluation of separate domain-general and domain-specific networks underlying different processes in WM. The results showed two domain-specific networks involved in stimulus encoding but not in other periods of WM. Two domain-general networks were also observed. The first domain-general network was involved in WM encoding, and the second, a domain-general attention network, was involved in attention processes in WM encoding, retrieval, and possibly maintenance as well. It seems likely that visual and auditory WM maintenance share a mechanism, in which the domain-general attention network directs attention to item-specific information stored elsewhere (cf. Lewis-Peacock & Postle, 2012), although domain-specific stores were not observed in this analysis. These results do not support the domain-specific account but favor the domain-general account that visual and auditory WM share a common maintenance mechanism, whereas existence of secondary domain-specific stores is also acknowledged (Cowan, 1995; Cowan et al., 2011; Harrison & Tong, 2009; Majerus et al., 2010). The interaction between domain-general and domain-specific networks and how this interaction supports WM maintenance, are questions that warrant further investigation.

Supplementary Material

Refer to Web version on PubMed Central for supplementary material.

Acknowledgments

This work was supported by NIH Grant R01 HD-21338 to Cowan. We thank Dr. Scott Saults for his assistance with the data collection.

References

Abe M, Hanakawa T, Takayama Y, Kuroki C, Ogawa S, Fukuyama H. Functional coupling of human prefrontal and premotor areas during cognitive manipulation. The Journal of Neuroscience. 2007; 27:3429–3438. doi:10.1523/JNEUROSCI.4273-06.2007. [PubMed: 17392459]

Baddeley, AD.; Hitch, GJ. Working memory. In: Bower, G., editor. Recent Advances in Learning and Motivation. Vol. 8. Academic Press; 1974.

Birn RM, Bandettini PA, Cox RW, Jesmanowicz A, Shaker R. Magnetic field changes in the human brain due to swallowing or speaking. Magnetic Resonance in Medicine. 2005; 40:55–60. doi: 10.1002/mrm.1910400108. [PubMed: 9660553]

Buckner RL, Andrews-Hanna JR, Schacter DL. The brain's default network: anatomy, function, and relevance to disease. Annals of the New York Academy of Sciences. 2008; 1124:1–38. doi:10.1196/annals.1440.011. [PubMed: 18400922]

Bush G, Luu P, Posner M. Cognitive and emotional influences in anterior cingulate cortex. Trends in Cognitive Sciences. 2000; 4:215–222. doi: 10.1016/S1364-6613(00)01483-2. [PubMed: 10827444]

Cairo, T. a; Liddle, PF.; Woodward, TS.; Ngan, ETC. The influence of working memory load on phase specific patterns of cortical activity. Cognitive Brain Research. 2004; 21:377–387. doi:10.1016/j.cogbrainres.2004.06.014. [PubMed: 15511653]

Camos V, Mora G, Oberauer K. Adaptive choice between articulatory rehearsal and attentional refreshing in verbal working memory. Memory & Cognition. 2011; 39:231–244. doi: 10.3758/s13421-010-0011-x. [PubMed: 21264630]

Chang C, Crottaz-Herbette S, Menon V. Temporal dynamics of basal ganglia response and connectivity during verbal working memory. Neuroimage. 2007; 34:1253–1269. doi:10.1016/j.neuroimage.2006.08.056. [PubMed: 17175179]

Chein JM, Moore AB, Conway ARA. Domain-general mechanisms of complex working memory span. Neuroimage. 2011; 54:550–559. doi:10.1016/j.neuroimage.2010.07.067. [PubMed: 20691275]

Cocchini G, Logie RH, Della Sala S, MacPherson SE, Baddeley AD. Concurrent performance of two memory tasks: evidence for domain-specific working memory systems. Memory & Cognition. 2002; 30:1086–1095. doi: 10.3758/BF03194326. [PubMed: 12507373]

Cohen J, Perlstein W, Braver T. Temporal dynamics of brain activation during a working memory task. Nature. 1997; 386:604–608. doi: 10.1038/386604a0. [PubMed: 9121583]

Cohen JR, Sreenivasan KK, D'Esposito M. Correspondence between stimulus encoding- and maintenance-related neural processes underlies successful working memory. Cerebral Cortex. 2012 doi:10.1093/cercor/bhs339.

Courtney SM, Ungerleider LG, Keil K, Haxby JV. Object and spatial visual working memory activate separate neural systems in human cortex. Cerebral Cortex. 1996; 6:39–49. doi: 10.1093/cercor/6.1.39. [PubMed: 8670637]

Cowan, N. Oxford Psychology Series. Oxford University Press; New York: 1995. Attention and memory: An integrated framework.

Cowan N, Li D, Moffit A, Becker TM, Martin EA, Saults JS, Christ SE. A neural region of abstract working memory. Journal of Cognitive Neuroscience. 2011; 23:2852–2863. doi: 10.1162/jocn.2011.21625. [PubMed: 21261453]

Culham JC, Kanwisher NG. Neuroimaging of cognitive functions in human parietal cortex. Current Opinion in Neurobiology. 2001; 11:157–163. doi: 10.1017/S0140525X01593929. [PubMed: 11301234]

Demonet JF, Chollet F, Ramsay S, Cardebat D, Nespoulous JL, Wise R, Rascol A, Frackowiak R. The anatomy of phonological and semantic processing in normal subjects. Brain. 1992; 115:1753–1768. doi: 10.1093/brain/115.6.1753. [PubMed: 1486459]

Edin F, Klingberg T. Mechanism for top-down control of working memory capacity. Proceedings of the National Academy of Sciences of the United States of America. 2009; 106:6802–6807. doi: 10.1073/pnas.0901894106. [PubMed: 19339493]

Edin F, Macoveanu J, Olesen P, Tegnér J, Klingberg T. Stronger synaptic connectivity as a mechanism behind development of working memory-related brain activity during childhood. Journal of

Cognitive Neuroscience. 2007; 19:750–760. doi:10.1162/jocn.2007.19.5.750. [PubMed: 17488202]

Fiebach CJ, Rissman J, D'Esposito M. Modulation of inferotemporal cortex activation during verbal working memory maintenance. Neuron. 2006; 51:251–261. doi:10.1016/j.neuron.2006.06.007. [PubMed: 16846859]

Gazzaley A, Rissman J, Cooney J, Rutman A, Seibert T, Clapp W, D'Esposito M. Functional interactions between prefrontal and visual association cortex contribute to top-down modulation of visual processing. Cerebral Cortex. 2007; 17(Suppl 1):i125–i135. doi:10.1093/cercor/bhm113. [PubMed: 17725995]

Gazzaley A, Rissman J, D'Esposito M. Functional connectivity during working memory maintenance. Cognitive, Affective & Behavioral Neuroscience. 2004; 4:580–599. doi: 10.3758/cabn.4.4.580.

Grill-Spector K, Kourtzi Z, Kanwisher N. The lateral occipital complex and its role in object recognition. Vision Research. 2001; 41:1409–1422. doi: 10.1016/S0042-6989(01)00073-6. [PubMed: 11322983]

Habeck C, Rakitin BC, Moeller J, Scarmeas N, Zarahn E, Brown T, Stern Y. An event-related fMRI study of the neural networks underlying the encoding, maintenance, and retrieval phase in a delayed-match-to-sample task. Cognitive Brain Research. 2005; 23:207–220. doi:10.1016/j.cogbrainres.2004.10.010. [PubMed: 15820629]

Habeck C, Rakitin B, Steffener J, Stern Y. Contrasting visual working memory for verbal and non-verbal material with multivariate analysis of fMRI. Brain Research. 2012; 1467:27–41. doi: 10.1016/j.brainres.2012.05.045. [PubMed: 22652306]

Hampson M, Driesen NR, Skudlarski P, Gore JC, Constable RT. Brain connectivity related to working memory performance. The Journal of Neuroscience. 2006; 26:13338–13343. doi:10.1523/JNEUROSCI.3408-06.2006. [PubMed: 17182784]

Hampson M, Driesen N, Roth JK, Gore JC, Constable RT. Functional connectivity between task-positive and task-negative brain areas and its relation to working memory performance. Magnetic Resonance Imaging. 2010; 28:1051–1057. doi:10.1016/j.mri.2010.03.021. [PubMed: 20409665]

Harrison SA, Tong F. Decoding reveals the contents of visual working memory in early visual areas. Nature. 2009; 458:632–635. doi:10.1038/nature07832. [PubMed: 19225460]

Haxby JV, Horwitz B, Ungerleider LG, Maisog JM, Pietrini P, Grady CL. The functional organization of human extrastriate cortex: a PET-rCBF study of selective attention to faces and locations. The Journal of Neuroscience. 1994; 14:6336–6353. [PubMed: 7965040]

Honey GD, Fu CHY, Kim J, Brammer MJ, Croudace TJ, Suckling J, Pich EM, Williams SCR, Bullmore ET. Effects of verbal working memory load on corticocortical connectivity modeled by path analysis of functional magnetic resonance imaging data. Neuroimage. 2002; 17:573–582. doi: 10.1006/nimg.2002.1193. [PubMed: 12377135]

Hunter MA, Takane Y. Constrained principal component analysis: Various applications. Journal of Educational and Behavioral Statistics. 2002; 27:105–145. doi: 10.3102/10769986027002105.

Kane MJ, Hambrick DZ, Tuholski SW, Wilhelm O, Payne TW, Engle RW. The generality of working memory capacity: a latent-variable approach to verbal and visuospatial memory span and reasoning. Journal of Experimental Psychology: General. 2004; 133:189–217. doi: 10.1037/0096-3445.133.2.189. [PubMed: 15149250]

Kim JS, Jung WH, Kang D-H, Park J-Y, Jang JH, Choi J-S, Choi C-H, Kim J, Kwon JS. Changes in effective connectivity according to working memory load: an FMRI study of face and location working memory tasks. Psychiatry Investigation. 2012; 9:283–292. doi:10.4306/pi.2012.9.3.283. [PubMed: 22993529]

Koelsch S, Schulze K, Sammler D, Fritz T, Müller K, Gruber O. Functional architecture of verbal and tonal working memory: an fMRI study. Human Brain Mapping. 2009; 30:859–873. doi:10.1002/hbm.20550. [PubMed: 18330870]

Kondo H, Morishita M, Osaka N, Osaka M, Fukuyama H, Shibasaki H. Functional roles of the cingulo-frontal network in performance on working memory. Neuroimage. 2004a; 21:2–14. doi: 10.1016/j.neuroimage.2003.09.046. [PubMed: 14741637]

Kondo H, Osaka N, Osaka M. Cooperation of the anterior cingulate cortex and dorsolateral prefrontal cortex for attention shifting. Neuroimage. 2004b; 23:670–679. doi:10.1016/j.neuroimage.2004.06.014. [PubMed: 15488417]

Kuo B-C, Yeh Y-Y, Chen AJ-W, D'Esposito M. Functional connectivity during top-down modulation of visual short-term memory representations. Neuropsychologia. 2011; 49:1589–1596. doi:10.1016/j.neuropsychologia.2010.12.043. [PubMed: 21241721]

Lacadie CM, Fulbright RK, Rajeevan N, Constable RT, Papademetris X. More accurate Talairach coordinates for neuroimaging using non-linear registration. NeuroImage. 2008; 42:717–725. doi:10.1016/j.neuroimage.2008.04.240. [PubMed: 18572418]

Lenartowicz A, McIntosh AR. The role of anterior cingulate cortex in working memory is shaped by functional connectivity. Journal of Cognitive Neuroscience. 2005; 17:1026–1042. doi:10.1162/0898929054475127. [PubMed: 16102235]

Lewis-Peacock JA, Postle BR. Decoding the internal focus of attention. Neuropsychologia. 2012; 50:470–478. doi:10.1016/j.neuropsychologia.2011.11.006. [PubMed: 22108440]

Ma L, Steinberg JL, Hasan KM, Narayana PA, Kramer LA, Moeller FG. Working memory load modulation of parieto-frontal connections: Evidence from dynamic causal modeling. Human Brain Mapping. 2012; 33:1850–1867. doi:10.1002/hbm.21329. [PubMed: 21692148]

Majerus S, D'Argembeau A, Martinez Perez T, Belayachi S, Van der Linden M, Collette F, Salmon E, Seurinck R, Fias W, Maquet P. The commonality of neural networks for verbal and visual short-term memory. Journal of Cognitive Neuroscience. 2010; 22:2570–2593. doi:10.1162/jocn.2009.21378. [PubMed: 19925207]

Mayer J, Roebroeck A. Specialization in the default mode: Task-induced brain deactivations dissociate between visual working memory and attention. Human Brain Mapping. 2009; 31:126–139. doi:10.1002/hbm.20850. [PubMed: 19639552]

Metzak PD, Feredoes E, Takane Y, Wang L, Weinstein S, Cairo T, Ngan ETC, Woodward TS. Constrained principal component analysis reveals functionally connected load-dependent networks involved in multiple stages of working memory. Human Brain Mapping. 2011; 32:856–871. doi:10.1002/hbm.21072. [PubMed: 20572208]

Metzak PD, Riley JD, Wang L, Whitman JC, Ngan ETC, Woodward TS. Decreased efficiency of task-positive and task-negative networks during working memory in schizophrenia. Schizophrenia Bulletin. 2012; 38:803–813. doi: 10.1093/schbul/sbq154. [PubMed: 21224491]

Mitchell DJ, Cusack R. Flexible, capacity-limited activity of posterior parietal cortex in perceptual as well as visual short-term memory tasks. Cerebral Cortex. 2008; 18:1788–1798. doi: 10.1093/cercor/bhm205. [PubMed: 18042643]

Nixon P, Lazarova J, Hodinott-Hill I, Gough P, Passingham R. The inferior frontal gyrus and phonological processing: an investigation using rTMS. Journal of Cognitive Neuroscience. 2004; 16:289–300. doi:10.1162/089892904322984571. [PubMed: 15068598]

Palva JM, Monto S, Kulashekhar S, Palva S. Neuronal synchrony reveals working memory networks and predicts individual memory capacity. Proceedings of the National Academy of Sciences of the United States of America. 2010; 107:7580–7585. doi:10.1073/pnas.0913113107. [PubMed: 20368447]

Payne L, Kounios J. Coherent oscillatory networks supporting short-term memory retention. Brain Research. 2009; 1247:126–132. doi:10.1016/j.brainres.2008.09.095. [PubMed: 18976639]

Petersen SE, Posner MI. The attention system of the human brain: 20 years after. Annual Review of Neuroscience. 2012; 35:73–89. doi:10.1146/annurev-neuro-062111-150525.

Posner MI, Petersen SE. The attention system of the human brain. Annual Review of Neuroscience. 1990; 13:25–42. doi:10.1146/annurev.ne.13.030190.000325.

Raye CL, Johnson MK, Mitchell KJ, Greene EJ, Johnson MR. Refreshing: A minimal executive function. Cortex. 2007; 43:135–145. [PubMed: 17334213]

Riggall AC, Postle BR. The relationship between working memory storage and elevated activity as measured with functional magnetic resonance imaging. The Journal of Neuroscience. 2012; 32:12990–12998. doi:10.1523/JNEUROSCI.1892-12.2012. [PubMed: 22993416]

Rissman J, Gazzaley A, D'Esposito M. Dynamic adjustments in prefrontal, hippocampal, and inferior temporal interactions with increasing visual working memory load. Cerebral Cortex. 2008; 18:1618–1629. doi:10.1093/cercor/bhm195. [PubMed: 17999985]

Ruchkin DS, Grafman J, Cameron K, Berndt RS. Working memory retention systems: a state of activated long-term memory. The Behavioral and Brain Sciences. 2003; 26:709–728. discussion 728–777. doi: 10.1017/S0140525X03000165. [PubMed: 15377128]

Saults JS, Cowan N. A central capacity limit to the simultaneous storage of visual and auditory arrays in working memory. Journal of Experimental Psychology. General. 2007; 136:663–684. doi: 10.1037/0096-3445.136.4.663. [PubMed: 17999578]

Schlösser RGM, Wagner G, Sauer H. Assessing the working memory network: Studies with functional magnetic resonance imaging and structural equation modeling. Neuroscience. 2006; 139:91–103. doi:10.1016/j.neuroscience.2005.06.037. [PubMed: 16324797]

Smith EE, Jonides J. Storage and executive processes in the frontal lobes. Science. 1999; 283:1657–1661. doi:10.1126/science.283.5408.1657. [PubMed: 10073923]

Sundermann B, Pfleiderer B. Functional connectivity profile of the human inferior frontal junction: involvement in a cognitive control network. BMC Neuroscience. 2012; 13:119. doi: 10.1186/1471-2202-13-119. [PubMed: 23033990]

Takane Y, Hunter MA. Constrained principal component analysis: A comprehensive theory. Applicable Algebra in Engineering, Communication and Computing. 2001; 12:391–419. doi: 10.1007/s002000100081.

Todd JJ, Marois R. Capacity limit of visual short-term memory in human posterior parietal cortex. Nature. 2004; 428:751–754. doi:10.1038/nature02466. [PubMed: 15085133]

Uddin LQ, Supekar K, Amin H, Rykhlevskaia E, Nguyen DA, Greicius MD, Menon V. Dissociable connectivity within human angular gyrus and intraparietal sulcus: evidence from functional and structural connectivity. Cerebral Cortex. 2010; 20:2636–2646. doi:10.1093/cercor/bhq011. [PubMed: 20154013]

Ungerleider LG, Courtney SM, Haxby JV. A neural system for human visual working memory. Proceedings of the National Academy of Sciences of the United States of America. 1998; 95:883–890. [PubMed: 9448255]

Van Essen DC. A population-average, landmark- and surface-based (PALS) atlas of human cerebral cortex. Neuroimage. 2005; 28:635–662. doi: 10.1016/j.neuroimage.2005.06.058. [PubMed: 16172003]

Van Essen DC, Dickson J, Harwell J, Hanlon D, Anderson CH, Drury HA. An integrated software system for surface-based analyses of cerebral cortex. Journal of American Medican Informatics Association. 2001; 8:443–459. doi: 10.1136/jamia.2001.0080443.

Van Essen DC, Dierker D. Surface-based and probabilistic atlases of primate cerebral cortex. Neuron. 2007; 56:209–225. doi: 10.1016/j.neuron.2007.10.015. [PubMed: 17964241]

Woodward TS, Cairo TA, Ruff CC, Takane Y, Hunter MA, Ngan ETC. Functional connectivity reveals load dependent neural systems underlying encoding and maintenance in verbal working memory. Neuroscience. 2006; 139:317–325. doi: 10.1016/j.neuroscience.2005.05.043. [PubMed: 16324799]

Woodward TS, Feredoes E, Metzak PD, Takane Y, Manoach DS. Epoch-specific functional networks involved in working memory. Neuroimage. 2013; 65:529–539. doi: 10.1016/j.neuroimage. 2012.09.070. [PubMed: 23041527]

Xu Y, Chun MM. Dissociable neural mechanisms supporting visual short-term memory for objects. Nature. 2006; 440:91–95. doi:10.1038/nature04262. [PubMed: 16382240]

Yetkin FZ, Haughton VM, Cox RW, Hyde J, Birn RM, Wong EC, Prost R. Effect of motion outside the field of view on functional MR. American Journal of Neuroradiology. 1996; 17:1005–1009. [PubMed: 8791907]

Highlights

- Working memory recruits both domain-general and domain-specific neural networks.
- Only a domain-general network shows load effects during working memory retention.
- The domain-general network includes part of the left anterior intrapanetal iulcus.
- We suggest that the intraparietal area's activity shows attention-related storage.
- Visual and verbal working memory share a common domain-general storage system.

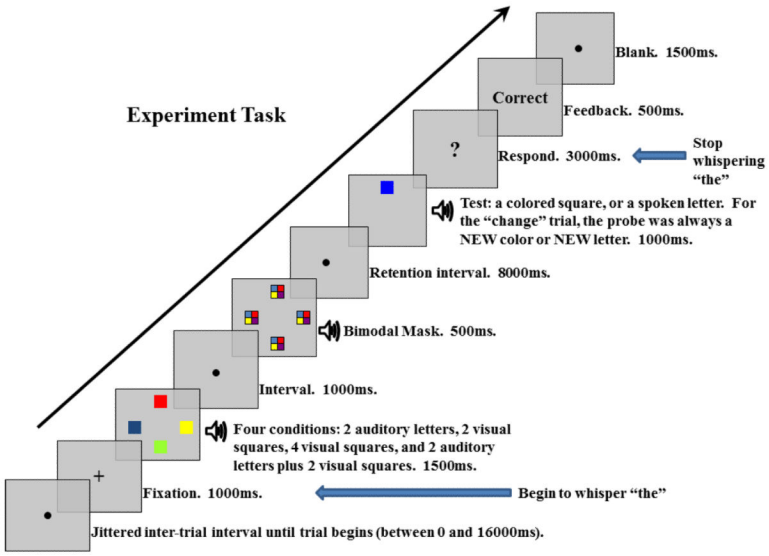

Figure 1.
Experimental procedure (after Cowan et al., 2011).

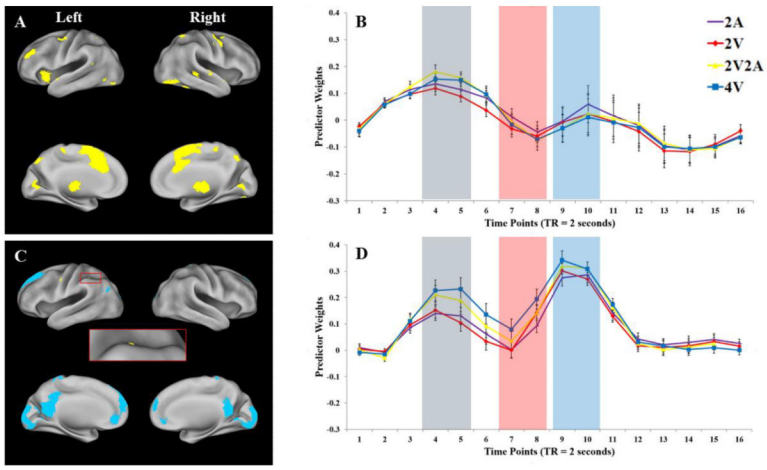

Figure 2.

Brain networks and predictor weights of two *domain-general* components (Components 1 and 3). A and C: brain regions of Components 1 and 3, respectively. The region in the red square in C shows the left anterior IPS. Only voxels with the most extreme 5% component loadings (whether positive or negative loadings) are displayed. Voxels with positive loadings are shown as yellow, and voxels with negative loadings are shown as blue. Results are visualized on an inflated PALS-B12 fiducial atlas (Van Essen, 2005; Van Essen & Dierker, 2007) provided by the Caret software (http://www.nitrc.org/projects/caret/; Van Essen et al., 2001). B and D: mean predictor weights over time (TR = 2 seconds) of Components 1 and 3, respectively. Red curve: 2 visual items (2V). Yellow curve: 2 visual and 2 auditory items (2V2A). Blue curve: 4 visual items (4V). The gray, red, and blue rectangles denote encoding, late maintenance, and response periods, respectively. The error bars represent standard error of the means.

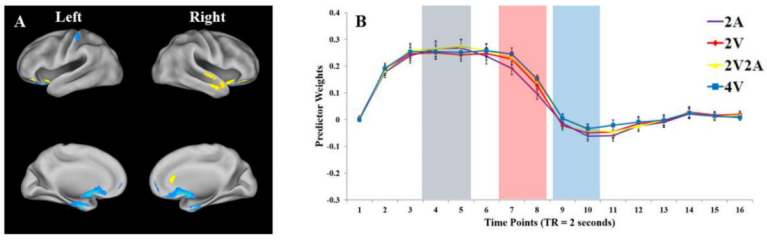

Figure 3.

Brain networks and predictor weights of Component 2. A: brain regions of Component 2. Only voxels with the most extreme 5% component loadings (whether positive or negative loadings) are displayed. Voxels with positive loadings are shown as yellow, and voxels with negative loadings are shown as blue. Results are visualized on an inflated PALS-B12 fiducial atlas (Van Essen, 2005; Van Essen & Dierker, 2007) provided by the Caret software (http://www.nitrc.org/projects/caret/; Van Essen et al., 2001). B: mean predictor weights over time (TR = 2 seconds) of Component 2. Purple curve: 2 auditory items (2A). Red curve: 2 visual items (2V). Blue curve: 4 visual items (4V). Yellow curve: 2 visual and 2 auditory items (2V2A). The yellow, red, and blue rectangles denote encoding, late maintenance, and response periods, respectively. The error bars represent standard errors.

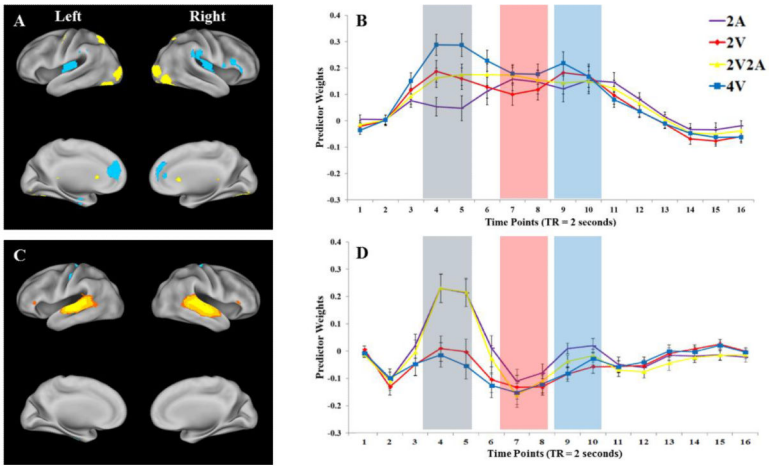

Figure 4.

Brain networks and predictor weights of two *domain-specific* components (Components 4 and 6). A and C: brain regions of Components 4 and 6, respectively. Only voxels with the most extreme 5% component loadings (whether positive or negative loadings) are displayed. Voxels with positive loadings are shown as yellow, and voxels with negative loadings are shown as blue. Results are visualized on an inflated PALS-B12 fiducial atlas (Van Essen, 2005; Van Essen & Dierker, 2007) provided by the Caret software (http://www.nitrc.org/projects/caret/; Van Essen et al., 2001). B and D: mean predictor weights over time (TR = 2 seconds) of Components 4 and 6, respectively. Red curve: 2 visual items (2V). Yellow curve: 2 visual and 2 auditory items (2V2A). Blue curve: 4 visual items (4V). The gray, red, and blue rectangles denote encoding, late maintenance, and response periods, respectively. The error bars represent standard error of the means.

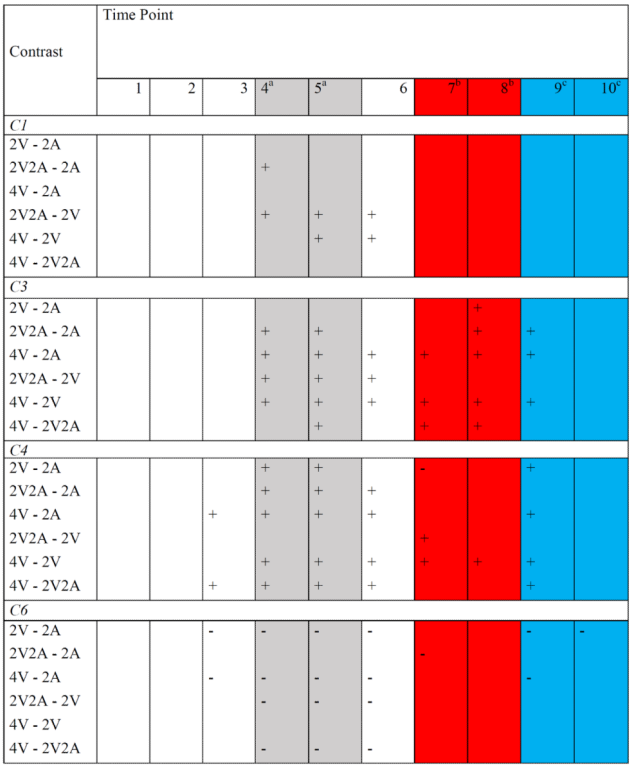

Contrast	Time Point									
	1	2	3	4[a]	5[a]	6	7[b]	8[b]	9[c]	10[c]
C1										
2V - 2A										
2V2A - 2A				+						
4V - 2A										
2V2A - 2V				+	+	+				
4V - 2V					+	+				
4V - 2V2A										
C3										
2V - 2A								+		
2V2A - 2A				+	+			+	+	
4V - 2A				+	+	+	+	+	+	
2V2A - 2V				+	+	+				
4V - 2V				+	+	+	+	+	+	
4V - 2V2A					+		+	+		
C4										
2V - 2A				+	+		-		+	
2V2A - 2A				+	+	+				
4V - 2A			+	+	+	+			+	
2V2A - 2V							+			
4V - 2V				+	+	+	+	+	+	
4V - 2V2A			+	+	+	+			+	
C6										
2V - 2A			-	-	-	-			-	-
2V2A - 2A							-			
4V - 2A			-	-	-	-			-	
2V2A - 2V				-	-	-				
4V - 2V										
4V - 2V2A				-	-	-				

Figure 5.

Significant Results of the Post-hoc Newman-Keuls Tests. C1, C3, C4, and C6 correspond to components 1, 3, 4, and 6, respectively. The rows are pairwise contrasts between WM load conditions. The columns are 10 time points, in which time point 1 refers to the onset of a trial (fixation). The "+" sign denotes a significant positive contrast, and the "−"sign denotes a significant negative contrast. 2V: 2 visual items. 2A: 2 auditory items. 4V: 4 visual items. 2V2A: 2 visual plus 2 auditory items. Time points 11–16 are not included in this figure, because these time points correspond mainly to the undershoot period of the hemodynamic function which does not carry a significant amount of task-related information. Very few contrasts were significant during this time period, the only ones being 2V-2A at time point 11 and 4V-2A at time points 11 and 12 in component 4. Both contrasts were negative. [a]encoding period, 4 and 5. blate maintenance period, 7 and 8. [c]response period, 9 and 10.

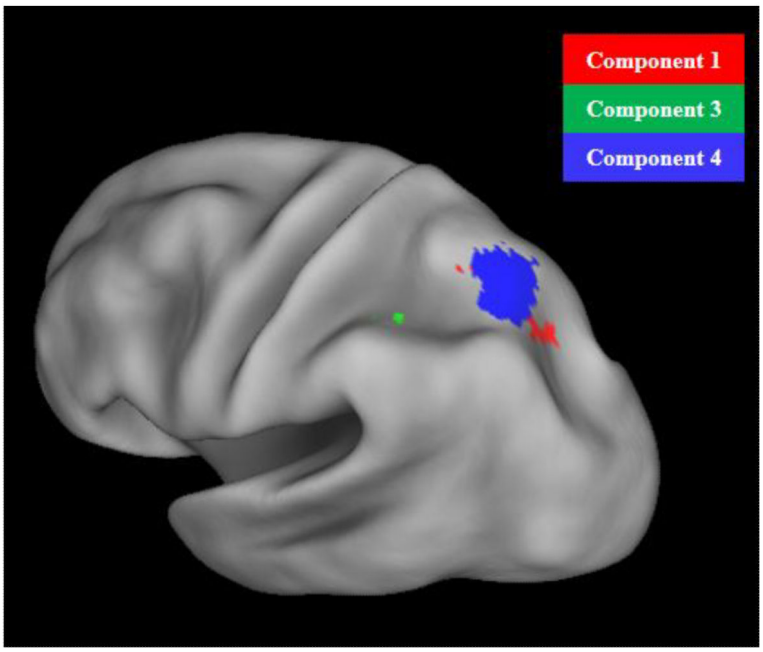

Figure 6.

Spatial locations of the IPS subregions found in Components 1, 3, and 4 in the left hemisphere. Red: the left IPS subregion in Component 1 (domain-general encoding). Green: the left IPS subregion in Component 3 (domain-general attention). Blue: the left IPS subregion in Component 4 (domain-specific visual encoding). The right IPS subregions in Component 1 and 3 showed similar spatial locations as their counterparts in the left hemisphere. Results are visualized on an inflated PALS-B12 fiducial atlas (Van Essen, 2005; Van Essen & Dierker, 2007) provided by the Caret software (http://www.nitrc.org/projects/caret/; Van Essen et al., 2001).